EXPERIMENTAL AND SIMULATED SCANNING TUNNELING MICROSCOPY OF THE CLEAVED $Rb_{1/3}WO_3$ (0001) SURFACE

WEIER LU AND GREGORY S. ROHRER
Carnegie Mellon University
Department of Materials Science and Engineering
Pittsburgh PA 15213

ABSTRACT

Atomic-scale resolution scanning tunneling microscope (STM) images of cleaved (0001) surfaces of the hexagonal tungsten bronze, $Rb_{1/3}WO_3$, show two distinct contrast patterns. We have interpreted these images using simulated constant current STM topographs. These simulations are constructed based on calculations of the tunnel current as a function of the lateral and vertical position above the surface. By calculating simulated images for the limiting cases of different termination layers, different tip sizes, and different electronic structures, it is possible to systematically explore the important parameters and choose a model that most closely matches the experimental observations. In this case, we conclude that two distinct termination layers have been imaged, a W-O terminated surface and a Rb-O terminated surface. Also, we have found that the O atoms on the W-O surface relax to new positions nearer the 6-fold axis of rotational symmetry. Some of the advantages and disadvantages of this model are discussed.

INTRODUCTION

The ability of the scanning tunneling microscope (STM) to record real-space, atomic-scale resolution images of metal oxide surfaces has been clearly demonstrated in recent publications [1-4]. However, experience shows that interpreting STM images from complex binary or ternary oxide surfaces can be considerably more challenging than recording the observations. Although the problem is somewhat simplified for the surfaces of two-dimensional materials that are formed by cleavage at a van der Waals gap [4], the quantitative interpretation of images from the surfaces of cleaved three-dimensionally bonded compounds is frustrated by uncertainties regarding the multiple termination layer possibilities, the inability to form images from both the bonding and anti-bonding bands (due to their large energy separation), uncertainties with respect to the electronic structure of the surface, and ill-defined tip structures [5].

We have recently reported experimental STM images of the cleaved (0001) surface of the hexagonal tungsten bronze (HTB), $Rb_{1/3}WO_3$ [5]. The structure of this compound, originally determined by Magnéli [6], is most easily visualized as a network of corner sharing WO_6 octahedral units, as shown in Fig. 1. In planes parallel to (0001), the octahedra link in a hexagonal pattern which leaves cavities in the structure. The layers are then stacked so that the cavities form tunnels parallel to the c axis and Rb ions occupy the 12-fold sites within the tunnels. Contrast in images of these surfaces, which exhibited two distinct patterns, was interpreted on the basis of qualitative arguments. We have assumed that variations in the termination layer are responsible for the different types of contrast. In the present paper, we attempt to quantify this interpretation and to learn more about the relationship between the surface atomic positions and the atomic-scale image contrast by simulating images within the framework of a simple model.

Mat. Res. Soc. Symp. Proc. Vol. 332. ©1994 Materials Research Society

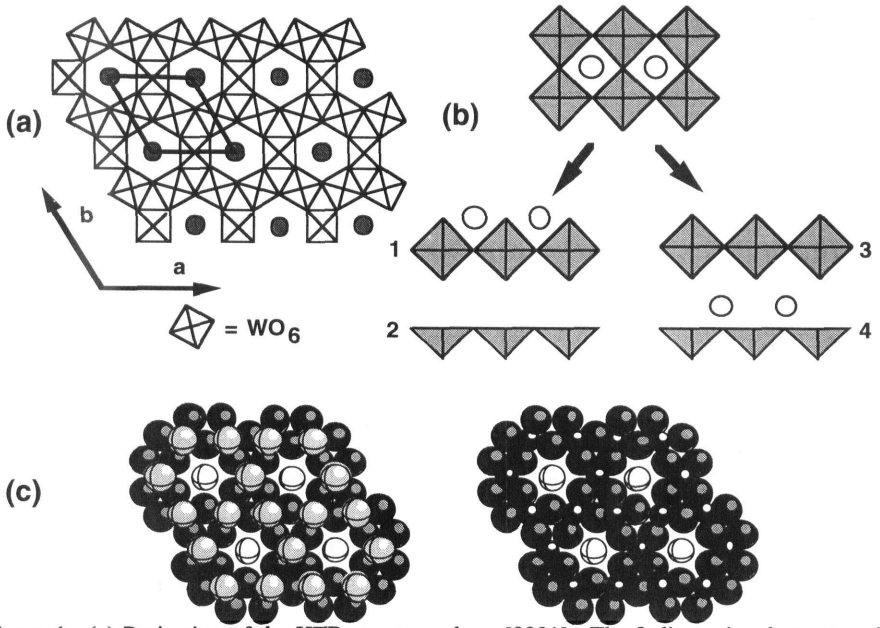

Figure 1. (a) Projection of the HTB structure along [0001]. The 3-dimensional structure is formed by stacking these layers so that each O at the apex of an octahedron is shared by one W above and one below. (b) When a corner-sharing network is broken, one surface consists of octahedra and the other of square pyramids. Depending on the fate of the alkali, there are four limiting cases. (c) Hard sphere models of the (0001) surface with apical O atoms in place (left) and with them, removed (right). The Rb are the spheres in the center of the rings, W are black, and the spheres representing O are shaded according to their height.

PROCEDURE

Fresh (0001) surfaces were formed by cleavage in air immediately before insertion into the vacuum chamber which had a base pressure of less than 1 X 10^{-9} torr. The tips used in these experiments were formed by clipping Pt-10% Ir wire and all of the images were acquired in the constant current mode using a 0.3 to 0.5 V sample bias (tunneling to unoccupied sample states) and a tunnel current of 0.6 to 0.8 nA. Details of the sample preparation and imaging can be found in ref. [5].

It is generally assumed that STM image contrast is determined primarily by the convolution of two factors: the surface electronic structure and the relative vertical positions of the surface atoms. In order to simulate these two effects within the framework of a simple, but physically valid model, we calculate the tunneling current as a function of the tip's lateral and vertical position over the sample assuming that each atom in the model contributes independently to the tunneling current and that at any specific coordinate, the tunneling current is given by a superposition of these contributions as follows.

$$I = \sum_i D_i \exp\left(-1.025\, S_i \sqrt{\phi}\right) \tag{1}$$

For the tunnel barrier height, ϕ, we used the value of 1.6 eV which was determined from an experimental measurement of the dependence of I on S_i. S_i is defined as the distance between the surface of the tip (a sphere with radius r_{tip}) and the surface of the i^{th} atom which is a hard sphere whose size is defined by the ionic radius. Although not explicitly in the equation for the tunneling current, the tip radius influences the current through its effect on the separations, S_i. D_i is the relative contribution of the i^{th} atom to the total density of electronic states in the conduction band (the band being probed in the STM images). This term is meant to represent, in the simplest possible way, the lateral variation of the surface density of states. For example, for a surface terminated by a single element, all D_i would be equal. For a binary surface layer, on the other hand, we would expect the density of conduction band states to be higher at the electropositive element and would weight the values of D_i appropriately. Once the current is determined at each position, constant current images can be easily extracted.

The computational simplicity of the model makes it is possible to generate many possible images based on different experimental parameters such as termination layer, atomic structure, tip size, and the contribution of each atom to the density of electronic states at the energy level being probed by the tip. Considering the fact that many of these parameters are ill-defined in most experiments, there is a considerable advantage to being able to systematically and rapidly explore the effects of the most important parameters.

The parameters that were found to have the most significant effect on the images are the termination layer, the relative contribution of the atoms to the band being probed by the STM (D_i), and the tip size (r_{tip}); choice of the constant current level or the barrier height influence only the total vertical corrugation and do not substantially alter the appearance of the image or the shapes of features, since images are normalized to maximize contrast. Our termination models are based on the fact that when the crystal is cleaved, only the longitudinal W-O bond that connects the apical oxygen anion and the W cation is broken. This creates four distinct limiting cases (illustrated schematically in Fig. 1b) based on the presence or absence of the apical O and the alkali atoms.

We considered two possible sets of values for D_i. The first is that all atoms contribute equally ($D_W = D_O = D_{Rb}$) and the second is that the values are weighted ($D_W = 9D_O = 90D_{Rb}$). We propose the weighting scheme based on the knowledge that the images were formed by tunneling to the conduction band and the assumption that this band is formed by the overlap of O 2p and W 5d orbitals and that Rb 5s orbitals make only a weak contribution. Although details of the electronic structure of this compound have not been studied, our numerical choices for the values of D_i were guided by the results of Bullett's [7] calculation of the electronic structure of cubic $NaWO_3$, a chemically similar compound.

RESULTS AND DISCUSSION

Figure 2 shows the two characteristic constant current STM images. Both have the hexagonal symmetry of the bulk structure and even preserve the bulk unit cell dimensions. However, the 6-fold symmetry axes of these two images are at contrary positions: at protrusions (white) in Fig. 2a and at depressions (black) in Fig. 2b. In the bulk structure, this axis of 6-fold rotational symmetry is located at the center of the hexagonal channel where the Rb cations reside. Thus, the point of 6-fold symmetry on the images must also represent this point.

Simulated images of the four possible termination layers, calculated under the assumption that the radius of the tip is equal to the radius of a Pt atom and that all of the D_i are equal, are shown in Fig. 3. The simulated images of the Rb-O (3a) terminated surface and of the Rb (3d) terminated surface both produce white contrast at the position of the 6-fold rotational axis and thus bear some resemblance to the experimental image in 2a. Of the two possibilities, we consider the simulated image of the Rb-O terminated surface to be the best match because the round areas of white contrast are approximately the same size as those in the

experimental image and there is some background gray contrast, as we also observe in the image.

None of the simulations in Fig. 3 produce the rings of white contrast that are characteristic of the experimental image in 2b. Assuming that the difference between the experimental image and the simulated images is due to the relaxation of the surface atoms to new positions, we note that on the W-O terminated surface (Fig. 3c), where O atoms create the bright contrast, the relaxation of these atoms toward the center of the tunnel could produce the characteristic rings of bright contrast while conserving the size of the surface repeat unit. A simulated image calculated under the same assumptions as in Fig 3c, but with the O atoms in sites displaced 0.3 Å toward the center of the tunnels, is shown in Fig 4a. A second calculation, using a tip with twice the radius of that in 4a is shown in 4b. Both images produce the characteristic white ring of contrast but it is the image in 4b that most closely resembles the experimental data in Fig. 2b.

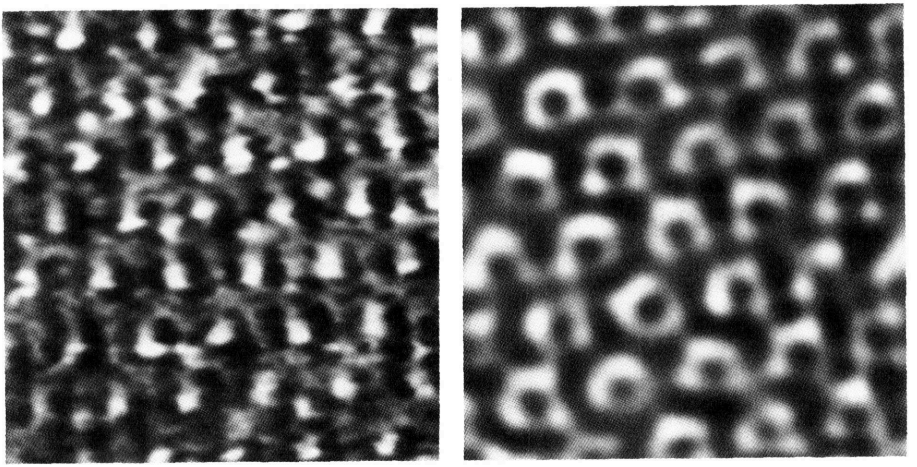

(a) (b)

Figure 2. 41 Å x 41 Å constant current STM images with a repeat unit equal to that of the bulk unit cell. (a) The vertical height (black-to-white contrast) is 2 Å. The raised white features are arranged in a pattern with 6-fold rotational symmetry. (b) The vertical height is 0.8 Å

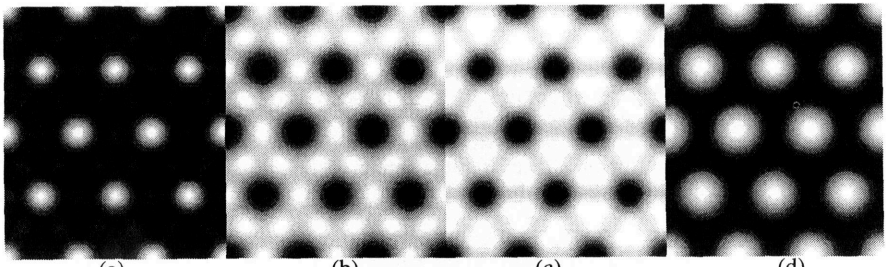

(a) (b) (c) (d)

Figure 3. Simulated STM images, 22 Å x 26 Å. (a) Rb-O surface, case 1 in Fig. 1b. (b) O surface, case 2 in Fig. 3. (c) W-O surface, case 3 in Fig. 1b. (d) Rb surface, case 4 in Fig. 1b. For all cases, $r_{tip} = r_{Pt} = 1.38$ Å and $D_W = D_O = D_{Rb}$

Based only on the simulations presented above, we would conclude that the image in 2a is of the Rb-O terminated surface and that the one in 2b is the W-O terminated surface, with

the surface O atoms in relaxed positions. It is, however, enlightening to consider other simulations using an alternate weighting scheme for the contribution of each atom to the surface density of states. Specifically, we assume that the contributions are weighted in such a way that $D_W = 9D_O = 90D_{Rb}$, values that seem chemically realistic assuming that polar-ionic bonding dominates in this material. Simulations of the Rb-O surface, the W-O surface with O atoms in relaxed positions, and the Rb terminated surface are shown in Fig. 5. We note that in the simulation of the Rb-O terminated surface the bright contrast is now dominated by the O atoms and that in the simulation of the W-O surface the bright contrast is now dominated by the W atoms position. Thus, using the weighted contributions, the simulated images of these surfaces no longer resemble any of the experimental images. On the other hand, in the simulated image of the Rb terminated surface, the size of the areas of white contrast shrink to sizes nearer those in Fig. 2a.

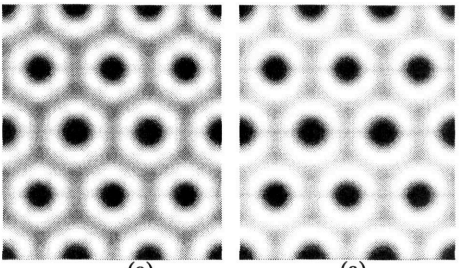

(a) (a)

Figure 4. Simulated images, 22 Å x 26 Å, of the W-O surface. (a) This is the same as Fig. 3c, but the O atoms occupy relaxed positions. (b) this is the same as a, but r_{tip} equals twice r_{Pt}.

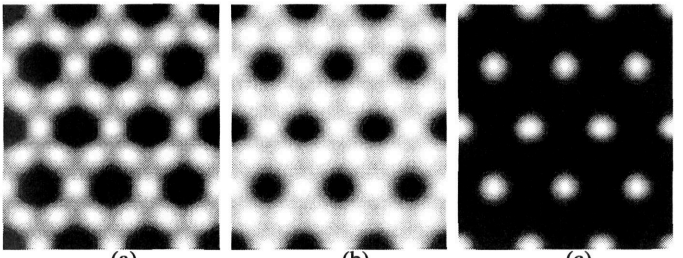

(a) (b) (c)

Figure 5. Simulated images, 22 Å x 26 Å, with $r_{tip} = r_{Pt} = 1.38$ Å and $D_W = 9D_O = 90D_{Rb}$. (a) The Rb-O surface. (b) The W-O surface. (c) The Rb surface.

The agreement between the experimental images and the simulated images is better when the contributions from all atoms are weighted equally. Although the reasons for this are not clear, we take this to be the appropriate model and conclude that Fig. 2a is an image of the Rb-O terminated surface and that Fig. 2b is an image of the W-O terminated surface with the atoms in relaxed positions. While it is possible that simulations which account for the lateral variations in the surface density of electronic states based on tight binding model calculations, which have been successfully used to interpret images of chalcogenides [8], might resolve this issue, we believe that our simplified model offers certain advantages. First, because of its simplicity, it allows a range of possible termination layers or surface structures to be easily examined. This is especially important for surfaces of complex ternary materials. Second, it includes effects related to the finite size of the tunneling tip, as shown in Fig. 4. As the tip gets larger, contributions from more and more tunneling sources become significant and affect the image contrast.

Finally, we comment on the O relaxation on the W-O surface. While this relaxation suggests unusually short O-O separations, they are nearly identical to the in-plane oxygen positions in the metastable hexagonal WO_3 which also has the HTB structure, but contains no alkali [9]. Thus, such a relaxation should not be unexpected because the surface layer can be viewed as a local approximation of the empty tunnel structure where at least half of the coordinating alkali atoms are missing. We also note that STM images of the cubic tungsten bronze $Na_{0.82}WO_3(100)$ surface demonstrated that surface atoms relaxed to form a 1x2 surface structure in response to the local ordering of sub-surface sodium [10]. These results, taken together with the results presented here, suggest that the alkali atoms play an important role in the determining how the surfaces of the tungsten bronzes relax.

CONCLUSION

Based on simulated constant current STM images of the hexagonal tungsten bronze $Rb_{1/3}WO_3$ (0001) surface, we conclude that different termination layers are responsible for the different types of contrast in the experimental images. Also, within the framework of our model, we conclude that the best agreement is obtained when it is assumed that all atoms contribute equally to the tunnel current. In other words, the effect of surface geometry dominates the effect of the local variations in the density of electronic states. Also, based on the simulations, we conclude that the O atoms on the W-O surface relax to positions closer to the six-fold symmetry axis. Based on a comparison to the structure of hexagonal WO_3, it seems that this relaxation is driven by broken alkali-oxygen bonds at the surface. While the results here suggest the need for more testing, we note that the proposed model provides tangible manifestations of the often used qualitative arguments regarding the origin of contrast in STM images and, because of its simplicity, provides some advantages for the interpretation of STM images from complex materials.

ACKNOWLEDGMENTS

This work was supported under National Science Foundation Grant DMR-9107305.

REFERENCES

[1] G. S. Rohrer, V. E. Henrich, and D. A. Bonnell, Science **250**, 1239 (1990).
[2] R. Wiesendanger, I. V. Shvets, D. Bürgler, G. Tarrach, H. J. Güntherodt, J. M. D. Coey, and S. Gräser, Science **255**, 583 (1992).
[3] T. Matsumoto, H. Tanaka, T. Kawai, and S. Kawai, Surface Science Letters, **278**, L153 (1992).
[4] G. S. Rohrer, W. Lu, R. L. Smith, and A. Hutchinson, Surface Science **292**, 261 (1993).
[5] W. Lu, N. Nevins, M. L. Norton, and G. S. Rohrer, Surface Science **291**, 395 (1993).
[6] A. Magnéli, Acta Chem. Scand. **7**, 315 (1953).
[7] D. W. Bullett, J. Phys. C: Solid State Phys. 16, 2197 (1983).
[8] J. Ren, M.-H. Whangbo, H. Bengel, H.-J. Cantlow, and S. N. Magonov, Chem. Mater. **5**, 1018 (1993).
[9] J. Oi, A. Kishimoto, and T. Kudo, J. Solid State Chem. **96**, 13 (1992).
[10] G. S. Rohrer, W. Lu, M. L. Norton, M. A. Blake, and C. L. Rohrer, in press J. Solid State Chemistry.